$\mathcal{H}_\infty$ Bipartite Synchronization of Double-Layer Markov Switched Cooperation-Competition Neural Networks: A Distributed Dynamic Event-Triggered Mechanism

Jing Wang, Mengping Xing, Jinde Cao, *Fellow, IEEE*, Ju H. Park, *Senior Member, IEEE*, and Hao Shen, *Member, IEEE*

***Abstract*— In this article, the $\mathcal{H}_\infty$ bipartite synchronization issue is studied for a class of discrete-time coupled switched neural networks with antagonistic interactions via a distributed dynamic event-triggered control scheme. Essentially different from most current literature, the topology switching of the investigated signed graph is governed by a double-layer switching signal, which integrates a flexible deterministic switching regularity, the persistent dwell-time switching, into a Markov chain to represent the variation of transition probability. Considering the coexistence of cooperative and antagonistic interactions among nodes, the bipartite synchronization of which the dynamics of nodes converge to values with the same modulus but the opposite signs is explored. A distributed control strategy based on the dynamic event-triggered mechanism is utilized to achieve this goal. Under this circumstance, the information update of the controller presents an aperiodic manner, and the frequency of data transmission can be reduced extensively. Thereafter, by constructing a novel Lyapunov function depending on both the switching signal and the internal dynamic nonnegative variable of the triggering mechanism, the exponential stability of bipartite synchronization error systems in the mean-square sense is analyzed. Finally, two simulation examples are provided to illustrate the effectiveness of the derived results.**

***Index Terms*— Cooperation-competition neural networks, double-layer Markov switching, distributed dynamic event-triggered mechanism, $\mathcal{H}_\infty$ bipartite synchronization, simultaneous structural balance.**

Manuscript received 6 September 2020; revised 15 January 2021 and 9 April 2021; accepted 25 June 2021. Date of publication 15 July 2021; date of current version 5 January 2023. This work was supported in part by the National Natural Science Foundation of China under Grant 61873002, Grant 61833005, Grant 61703004, and Grant 61973199; in part by the Fundamental Research Funds for the Central Universities, in part by the Major Natural Science Foundation of Higher Education Institutions of Anhui Province under Grant KJ2020ZD28; and in part by the Major Technologies Research and Development Special Program of Anhui Province under Grant 202003a05020001. The work of Ju H. Park was supported by the National Research Foundation of Korea (NRF) grant funded by the Korean government (MSIT) under Grant 2020R1A2B5B02002002. *(Corresponding authors: Ju H. Park and Hao Shen.)*

Jing Wang is with the Anhui Province Key Laboratory of Special Heavy Load Robot, Ma'anshan 243032, China, and also with the School of Electrical and Information Engineering, Anhui University of Technology, Ma'anshan 243002, China (e-mail: jingwang08@126.com).

Mengping Xing is with the School of Cyber Science and Engineering, Southeast University, Nanjing 210096, China (e-mail: 13856079203@163.com).

Jinde Cao is with the School of Mathematics, Southeast University, Nanjing 210096, China, and also with the Yonsei Frontier Lab, Yonsei University, Seoul 03722, South Korea (e-mail: jdcao@seu.edu.cn).

Ju H. Park is with the Department of Electrical Engineering, Yeungnam University, Gyeongsan 38541, Republic of Korea (e-mail: jessie@ynu.ac.kr).

Hao Shen is with the School of Electrical and Information Engineering, Anhui University of Technology, Ma'anshan 243002, China, and also with the Key Laboratory of Smart Manufacturing in Energy Chemical Process, Ministry of Education, East China University of Science and Technology, Shanghai 200237, China (e-mail: haoshen10@gmail.com).

Color versions of one or more figures in this article are available at https://doi.org/10.1109/TNNLS.2021.3093700.

Digital Object Identifier 10.1109/TNNLS.2021.3093700

I. Introduction

IN THE past several decades, neural networks (NNs) involving complicated interactions among intricately connected nodes have stimulated intense interests from academic communities due to their inherent advantages and potential applications in artificial intelligence [1], pattern recognition [2], secure communication [3], and some other fields [4]–[10]. In general, the interconnection of dynamical nodes composing NNs exhibits particular topology, which characterizes the information interaction among various neurons. When the interactions among nodes are considered to be mutually collaborative, which corresponds to nonnegative graphs, relevant issues have been extensively studied, and tremendous developments have been achieved [11]–[13]. However, in many practical scenarios, networks involving both cooperative and antagonistic interactions among nodes are ubiquitous [14]–[16]. Taking social networks as an example, the associated relationships among different individuals generally include trust/distrust, friendly/hostile, like/dislike, and so on [17]. To characterize these situations, the signed graph that uses positive and negative weights to describe these two opposite relationships is widely adopted. Considering the practical significance of cooperation-competition networks and the solid theoretical support from the graph theory, it is not surprising that many representative works have emerged in recent years. In terms of the structurally balanced concept, some essential properties of networks with antagonistic interactions were explored in the pioneering work of Altafini [18]. In [19], the bipartite consensus problem for a group of high-order multiagents was discussed, where the structurally balanced signed graph with fixed topology was investigated. Following this research line, the consensus/synchronization problems of systems subject to cooperation-competition interactions were discussed in [20]–[22]. Under a relatively relaxed restriction on the topology that the signed digraphs only contain spanning trees, the interval bipartite consensus issue was further studied in [23].

In most practical scenarios, the interaction among nodes may change over time or state, which means that the weighted signed graph may possess switching property [24]–[27]. Thus, another research direction about networks with switching topologies has recently been the research hotspot of many scholars. Based on the tracker information, the synchronization problem for discrete-time NNs with Markov jump topologies was investigated in [28]. Recently, inspired by Liu and Chen [29], multiagent systems subject to stochastic switching topologies were discussed in [30]. Furthermore, specific to systems with antagonistic interactions and switching topologies, the consensus and synchronization issues were explored in [31] and [32], respectively. It can be noticed that the developed results on Markov jump NNs are mainly based on an implicit constraint, i.e., switching characteristic of the topology can be described by a perfect Markov chain, which may fail to cover all situations yet, especially in the circumstance that the transition probabilities (TPs) of the Markov chain are sensitive to certain interference and, therefore, exhibit the time-varying characteristic. In light of this situation, the concept of a nonhomogeneous Markov chain has been introduced to cope with relevant issues. Corresponding research results can be found in [33]–[35], where the piecewise homogeneous TPs of the Markov chain were supposed to be subject to arbitrary switching, dwell-time switching, and average dwell-time switching regularities, respectively. These pioneering works have provided a solid theoretical foundation for follow-up studies. Furthermore, achievements presented in [36] have certified that the switching regularity of persistent dwell-time (PDT) is more general than dwell time and average dwell-time switching regularities as the former can degrade into the latter two forms by selecting specific parameters. Therefore, extending relevant studies to Markov jump cooperation-competition NNs subject to PDT switched TPs is of great significance, which has currently not been fully researched yet due perhaps to the relatively intractable analysis process.

Furthermore, in terms of the switched cooperation-competition NNs, investigating the complete synchronization of all nodes is unrealistic due to the competitive behaviors among nodes. Thus, the bipartite synchronization, which requires that nodes belonging to one subgraph converge to a reference state, while nodes of the other subgraph converge to the opposite value of the reference, has been intensively studied. To achieve the bipartite synchronization of networks with antagonistic interactions, scholars have spared no effort to explore various available control strategies, and many remarkable studies have been reported including but not limited to pinning control and adaptive control [14], [32]. Moreover, in consideration of the constrained communication bandwidth, data transmission through shared networks usually suffers from data congestion or collision. In this circumstance, the event-triggered communication scheme that carries out data transmission only when a certain condition is violated can be one of the optimal choices, as it can alleviate the transmission burden of networks by reducing the frequency of data transmission. With this superiority, some interesting issues have been discussed in [37]–[41], and references therein. Very recently, by constructing an internal dynamic nonnegative variable based on the behavior of the underlying system, Girard [42] proposed a novel dynamic event-triggered mechanism that can further reduce the transmission frequency compared to the static one. Significant extensions can be found in [43]–[45]. Although the dynamic event-triggered mechanism has shown conspicuous advantages, relevant studies based on distributed control schemes have not yet received enough attention, let alone taken NNs subject to antagonistic interactions and switching topologies into account simultaneously.

Motivated by the above observations, this article centers on investigating the $\mathcal{H}_\infty$ bipartite synchronization issue for double-layer switched cooperation-competition NNs under the distributed dynamic event-triggered (DDET) control scheme. The main contributions are identified in the following three aspects.

1) The double-layer switching signal, which integrates the PDT switching into a Markov chain to represent the variation of transition probability, is introduced for the first attempt to the analysis of cooperation-competition NNs to describe the switching of the signed weighted topology.
2) In the discrete-time context, a DDET controller is designed in terms of linear matrix inequalities. With the aid of the developed control strategy, the bipartite synchronization of the investigated NNs can be realized at an exponential convergence rate in the mean-square sense. Meanwhile, the frequency of data transmission can be significantly reduced via the employed dynamic event-triggered mechanism.
3) A novel model synthesizing both the coupled switched NNs with antagonistic interactions and the DDET transmission mechanism is established. Adequate simulation results, including the analysis of the dynamic behavior of chaotic networks and the influence of the DDET mechanism, are provided.

Notations: The notations used in this article are standard except otherwise stated. "$\otimes$" denotes the Kronecker product. $\mathbf{1}_N$ and I_n stand for a column vector with all entries being 1 and an identity matrix, respectively. $\mathbb{R}^a$ and $\mathbb{R}^{a\times b}$ severally represent the a-dimensional Euclidean space and the set of $a \times b$-dimensional matrices. $\mathbb{Z}_+$ signifies the set of nonnegative integers. A^T means the transpose of matrix A, and sym(A) means $A + A^T$. diag$\{\ldots\}$ signifies the block-diagonal matrix. The expectation operator is represented by $\mathcal{E}\{\cdot\}$. "$*$" denotes the term induced by symmetry. sgn$(\cdot)$ signifies the sign function. For a symmetric matrix, $A > 0(\geq 0)$ describes positive (semipositive) definite matrix. $\vec{\lambda}_{\min}(A)(\vec{\lambda}_{\max}(A))$ means the smallest (largest) eigenvalue of matrix A.

II. Problem Formulation and Preliminaries

A. Interaction Graph

Before further presenting, some necessary preliminaries of algebraic graph theory [46] are presented.

The neural network is composed of N coupled neuron nodes, and the interactions among nodes are described by the weighted signed graph $\mathcal{G}^{\eta(k)} \triangleq (\mathcal{N}, \Im^{\eta(k)}, \mathcal{H}^{\eta(k)})$, which is subject to the switching topology, with $\eta(k) \in \mathcal{R} \triangleq \{1, 2, \ldots, R\}$ being the switching signal. $\mathcal{N} \triangleq \{1, 2, \ldots, N\}$ is the set of nodes; $\Im^{\eta(k)} \subseteq \mathcal{N}\times\mathcal{N}$ and $\mathcal{H}^{\eta(k)} \triangleq [h_{ij}^{\eta(k)}]_{N\times N}$ denote the edge set and the weighted adjacent matrix under the topology $\eta(k)$, respectively. Since the antagonistic interactions are considered among nodes, the collaborative and antagonistic behaviors are represented by edges with positive and negative weights, respectively. Specifically, directed against the topology $\eta(k)$, the entry $h_{ij}^{\eta(k)} > 0$ ($h_{ij}^{\eta(k)} < 0$) means that node i can receive information from node j, and $(j, i) \in \Im^{\eta(k)}$ is the positive (negative) edge. $h_{ij}^{\eta(k)} = 0$ signifies $(j, i) \notin \Im^{\eta(k)}$. Besides, the self-loop (i, i) is not allowed, i.e., $h_{ii}^{\eta(k)} = 0$ $\forall\eta(k) \in \mathcal{R}$, $i \in \mathcal{N}$.

The degree of node i under the topology $\eta(k)$ is denoted as $\tilde{d}_i^{\eta(k)} = \sum_{j=1}^{N} |h_{ij}^{\eta(k)}|$. Then, the Laplacian matrix $\mathcal{L}^{\eta(k)} \triangleq [l_{ij}^{\eta(k)}]_{N\times N}$ of graph $\mathcal{G}^{\eta(k)}$ can be given by

$$\mathcal{L}^{\eta(k)} = \mathcal{D}^{\eta(k)} - \mathcal{H}^{\eta(k)} \tag{1}$$

where $\mathcal{D}^{\eta(k)} \triangleq \mathrm{diag}\{\tilde{d}_1^{\eta(k)}, \tilde{d}_2^{\eta(k)}, \ldots, \tilde{d}_N^{\eta(k)}\}$.

Definition 1 [31]: The weighted signed graph $\mathcal{G}^{\eta(k)}(\eta(k) \in \mathcal{R})$ is simultaneously structurally balanced if the node set $\mathcal{N}$ can be uniformly divided into two disjoint subsets $\mathcal{N}_1$ and $\mathcal{N}_2$, i.e., $\mathcal{N}_1 \cup \mathcal{N}_2 = \mathcal{N}$ and $\mathcal{N}_1 \cap \mathcal{N}_2 = \varnothing$, such that $h_{ij}^{\eta(k)} \geq 0$ $\forall i, j \in \mathcal{N}_\upsilon (\upsilon \in \{1, 2\})$ $\forall\eta(k) \in \mathcal{R}$, and $h_{ij}^{\eta(k)} \leq 0$ $\forall i \in \mathcal{N}_\upsilon$, $j \in \mathcal{N}_w, i \neq j (\upsilon, w \in \{1, 2\})$ $\forall\eta(k) \in \mathcal{R}$. Otherwise, $\mathcal{G}^{\eta(k)}$ is simultaneously structurally unbalanced.

Lemma 1 [18], [31]: If the weighted signed graph $\mathcal{G}^{\eta(k)}(\eta(k) \in \mathcal{R})$ is simultaneously structurally balanced, there will exist a gauge transformation matrix $\Psi \triangleq \mathrm{diag}\{\psi_1, \psi_2, \ldots, \psi_N\}$ ($\psi_i \in \{1, -1\}, i \in \mathcal{N}$), which satisfies $\vec{\mathcal{H}}^{\eta(k)} = \Psi\mathcal{H}^{\eta(k)}\Psi$ with $\vec{\mathcal{H}}^{\eta(k)} \triangleq [|h_{ij}^{\eta(k)}|]_{N\times N}$ $\forall\eta(k) \in \mathcal{R}$.

Remark 1: Considering that the value of the connected weight of a graph may change over time in many practical scenarios, thus, a switching signal $\eta(k)$ is duly introduced to describe the variation of the topology. Moreover, if the set $\mathcal{R}$ contains only one element, the topology under consideration will degrade into the nonswitching case. For any $\eta(k) \in \mathcal{R}$, it can be noted that the Laplacian matrix $\mathcal{L}^{\eta(k)}$ is not a zero-row-sum matrix, which makes relevant analyses more difficult than these of traditional unsigned graphs. Thus, Lemma 1 concerning the transformation matrix Ψ is introduced in this article. It should be mentioned that, for networks with switching topology, the simultaneously structurally balanced concept in Definition 1 ensures that the graph sequence $\{\mathcal{G}^1, \mathcal{G}^2, \ldots, \mathcal{G}^R\}$ is sign consistent, and the requirement that the entries of $\Psi\mathcal{H}^{\eta(k)}\Psi$ are all nonnegative can be satisfied under a unified gauge transformation matrix Ψ $\forall\eta(k) \in \mathcal{R}$. From the above statements, it is not difficult to find that $\vec{\mathcal{L}}^{\eta(k)} = \Psi\mathcal{L}^{\eta(k)}\Psi = [\vec{l}_{ij}^{\eta(k)}]_{N\times N}$ is a zero-row-sum matrix for each $\eta(k) \in \mathcal{R}$, which will be utilized subsequently.

B. Node Dynamics With Switching Topology

Considering the coupled NNs with antagonistic interactions and double-layer switching topologies, the dynamics of node i are presented as follows:

$$\begin{aligned} x_i(k+1) &= Ax_i(k) + Bf(x_i(k)) + u_i(k) + E_i\varpi(k) \\ &\quad + c\sum_{j=1}^{N} \left|h_{ij}^{\eta(k)}\right|\left(\mathrm{sgn}\left(h_{ij}^{\eta(k)}\right)x_j(k) - x_i(k)\right) \\ z_i(k) &= F\psi_i x_i(k), \quad i = 1, 2, \ldots, N \end{aligned} \tag{2}$$

where $x_i(k) \triangleq [x_{i1}(k), x_{i2}(k), \ldots, x_{in}(k)]^T \in \mathbb{R}^n$, $u_i(k) \in \mathbb{R}^{n_u}$, and $z_i(k) \in \mathbb{R}^{n_z}$ are the state, control input, and output vectors of node i, respectively. $\varpi(k) \in \mathbb{R}^{n_\varpi}$ denotes the disturbance input belonging to $l_2[0, \infty)$. $f(x_i(k)) \triangleq [f_1(x_{i1}(k)), f_2(x_{i2}(k)), \ldots, f_n(x_{in}(k))]^T \in \mathbb{R}^n$ represents the neuron activation functions. $c \in (0, \infty)$ signifies the coupling strength. $A \triangleq \mathrm{diag}\{a_1, a_2, \ldots, a_n\} \in \mathbb{R}^{n\times n}$, $B \in \mathbb{R}^{n\times n}$, $E_i \in \mathbb{R}^{n\times n}$, and $F \in \mathbb{R}^{n_z\times n}$ are known constant matrices with compatible dimensions.

For the probability space $(\tilde{\mathcal{F}}, \tilde{\Gamma}, \mathrm{Pr})$, $\{\eta(k), k \in \mathbb{Z}_+\}$ denotes a Markov chain, which is a right-continuous function taking values in the fixed set $\mathcal{R}$. It is utilized to describe the switching of the topology. Since the TPs of the Markov chain are considered to be piecewise constants, the transition probability matrix (TPM) can be given as $\hat{\Lambda}^{\sigma(k)} \triangleq [\tilde{\pi}_{r_1r_2}^{\sigma(k)}]_{R\times R}$, where

$$\tilde{\pi}_{r_1r_2}^{\sigma(k)} \triangleq \mathrm{Pr}\{\eta(k+1) = r_2|\eta(k) = r_1\} \tag{3}$$

with $\tilde{\pi}_{r_1r_2}^{\sigma(k)} \in [0, 1]$ $\forall r_1, r_2 \in \mathcal{R}$, $k \in \mathbb{Z}_+$, and $\sum_{r_2=1}^{R} \tilde{\pi}_{r_1r_2}^{\sigma(k)} = 1$ $\forall r_1 \in \mathcal{R}$. In detail, $\tilde{\pi}_{r_1r_2}^{\sigma(k)}$ means the probability that the system topology jumps from mode r_1 at current sampling instant k to mode r_2 at next sampling instant $k+1$. The determination of the TPs is relevant to the current moment k. Specifically, the variation of the probability along time is governed by a right-continuous piecewise constant function $\sigma(k)$, which satisfies the PDT switching regularity. Furthermore, it is supposed that the signal $\sigma(k)$ takes values in a predetermined set, i.e., $\sigma(k) \in \mathcal{Q} \triangleq \{1, 2, \ldots, Q\}$. To elaborate on the PDT switching rule, the following relevant concepts are introduced.

Definition 2 [36]: For scalars $\tau_P > 0$ (the persistent dwell time) and $T_P > 0$ (the period of persistence), the signal $\sigma(k)$ complies with PDT switching rule if the following constraints are satisfied.

1) $\sigma(k)$ takes values as a constant in a series of nonadjacent intervals with length no smaller than τ_P.
2) For the segments located in the abovementioned intervals, $\sigma(k)$ can take different values, and the duration of each value is less than τ_P, while the overall duration is no more than T_P.

Remark 2: The total switching times of the PDT switching signal $\sigma(k)$ in the interval $(k_1, k_2]$ are denoted as $\Omega(k_1, k_2)$, which satisfies [33]

$$\Omega(k_1, k_2) < [(k_2 - k_1)/(T_P + \tau_P) + 1](T_P + 1). \tag{4}$$

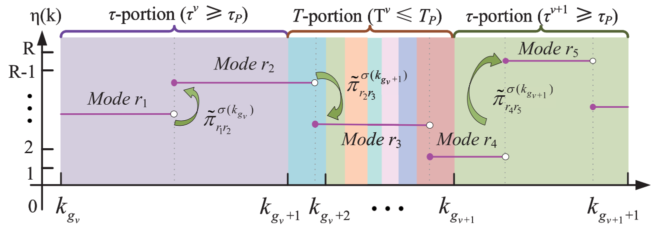

Fig. 1. Possible switching sequence of $\{\eta(k), k \in [k_{g_\upsilon}, k_{g_{\upsilon+1}+1})\}$ under PDT switching regularity.

Furthermore, it can be noted from Definition 2 that the PDT switching signal $\sigma(k)$ can be described in a series of stages. Each stage consists of a τ-portion and a T-portion. Taking the υth stage as an example (as depicted in Fig. 1), the actual length of τ-portion is $\tau^\upsilon(\tau^\upsilon \geq \tau_P)$, and the actual length of T-portion is $T^\upsilon = T^{(\upsilon_1)} + T^{(\upsilon_2)} + \cdots + T^{(\upsilon_{\Omega(\upsilon)})}(T^\upsilon \leq T_P)$, where $\Omega(\upsilon)$ signifies the switching times of $\sigma(k)$ in the T-portion of the υth stage. In the τ-portion, $\sigma(k)$ is a constant, while, in the T-portion, $\sigma(k)$ can take different values at different time periods. To facilitate the follow-up analysis, the switching times sequence of $\sigma(k)$ is denoted as $\{k_{g_1}, k_{g_1+1}, k_{g_1+2}, \ldots, k_{g_1+\Omega(1)}, \ldots, k_{g_\upsilon}, k_{g_\upsilon+1}, \ldots, k_{g_\upsilon+\Omega(\upsilon)}, \ldots\}$. Moreover, the possible jumping sequence $\{\eta(k), k \in [k_{g_\upsilon}, k_{g_{\upsilon+1}+1})\}$ is also presented in Fig. 1.

Remark 3: In this article, the topology variation is embodied in $h_{ij}^{\eta(k)}$, of which $\eta(k)$ denotes a double-layer switching signal. It is obvious that this signal integrates the random characteristic of the stochastic Markov jump sequence with the flexibility merits (describe the intermittent occurrence of slow and fast events in a uniform framework in terms of the property of the τ-portion and T-portion) of the deterministic PDT switching rule. Moreover, it can be noted that the double-layer switching can be degraded into traditional Markov jump case by considering $\tau_P \to \infty$ when the PDT switching sequence starts from τ-portion or takes $\mathcal{Q} \triangleq \{1\}$ directly. It means that the adopted switching description model is more comprehensive.

Before further presentation, some assumptions about signed graph $\mathcal{G}^{\eta(k)}$ and activation function $f(\cdot)$ are provided.

Assumption 1: The signed graph $\mathcal{G}^{\eta(k)}, \eta(k) \in \mathcal{R}$ of neural network (2) is simultaneously structurally balanced.

Assumption 2: For $i = 1, 2, \ldots, n$, $f_i(a) : \mathbb{R} \mapsto \mathbb{R}$ is a bounded and odd activation function, which satisfies

$$\tau_i^- \leq \frac{f_i(a) - f_i(b)}{a - b} \leq \tau_i^+, \quad a \neq b \tag{5}$$

where $f_i(0) = 0$. τ_i^- and τ_i^+ are known real constants that can be taken as positive, zero, or negative.

The dynamic of the unforced isolated node corresponding to neural network (2) is presented as follows:

$$\begin{aligned} s(k+1) &= As(k) + Bf(s(k)) \\ \bar{z}(k) &= Fs(k) \end{aligned} \tag{6}$$

where $s(k) \triangleq [s_1(k), s_2(k), \ldots, s_n(k)]^T \in \mathbb{R}^n$ and $\bar{z}(k) \in \mathbb{R}^{n_z}$ are the state and output vectors of the isolated node, respectively. Other symbols are consistent with (2).

For simplicity, we consider the following abridged notations: $\hat{\Lambde}^{\sigma(k)} \triangleq \hat{\Lambda}^{q_1}$ and $\mathcal{H}^{\eta(k)} \triangleq \mathcal{H}^{r_1}$ $\forall \sigma(k) = q_1,\ \eta(k) = r_1$, and other symbols are similarly defined. Then, based on Lemma 1, matrix Ψ is employed for vector transformation. Denote $\tilde{x}_i(k) \triangleq \psi_i x_i(k), i = 1, 2, \ldots, N$. Since $\vec{\mathcal{L}}^{r_1} \triangleq \Psi \mathcal{L}^{r_1} \Psi$ is a zero-row-sum matrix for each $r_1 \in \mathcal{R}$, the coupled switched NNs can be further depicted as

$$\begin{aligned} \tilde{x}_i(k+1) &= A\tilde{x}_i(k) + Bf(\tilde{x}_i(k)) + \psi_i u_i(k) \\ &\quad - c\sum_{j=1}^N \vec{l}_{ij}^{r_1} \tilde{x}_j(k) + \psi_i E_i \varpi(k) \\ z_i(k) &= F\tilde{x}_i(k), \quad i = 1, 2, \ldots, N. \end{aligned} \tag{7}$$

C. Distributed Dynamic Event-Triggered Controller

For the purpose of mitigating the communication burden, inspired by Girard [42], a DDET mechanism is employed to determine the instant of data transmission and update the input signal of the controller. Furthermore, the bipartite synchronization error is defined as $e_i(k) \triangleq \tilde{x}_i(k) - s(k)$, which will be utilized for the controller design subsequently. The sequence $\{k_i^m | m \in \mathbb{Z}_{\geq 0}\}$ represents the set of event-triggered instants of the ith neuron node. $\forall i \in \mathcal{N}$, when the current event-triggered instant is k_i^m, then the next triggering instant k_i^{m+1} can be determined aperiodically by the following event-triggered mechanism:

$$\begin{aligned} k_i^{m+1} &= \inf\big\{k \in \mathbb{Z}_+ \big| k > k_i^m, \text{ and } \delta_i(k) \\ &\quad + \theta_i(\vartheta_i e_i^T(k)e_i(k) - \zeta_i^T(k)\zeta_i(k)) \leq 0\big\} \end{aligned} \tag{8}$$

$$\delta_i(k+1) = \varrho_i \delta_i(k) + \vartheta_i e_i^T(k)e_i(k) - \bar{\zeta}_i^T(k)\bar{\zeta}_i(k) \tag{9}$$

where $\theta_i \in (0, \infty)$, $\vartheta_i \in (0, \infty)$, and $\varrho_i \in (0, 1)$ are known scalars. For $k \in (k_i^m, k_i^{m+1}]$, $\zeta_i(k) \triangleq e_i(k) - e_i(k_i^m)$ denotes the measurement error. Correspondingly, $\bar{\zeta}_i(k)$ is defined as $\bar{\zeta}_i(k) \triangleq e_i(k) - e_i(k_i^m)$ with

$$k_i^m \triangleq \sup\big\{k_i^{\bar{m}} \big| k_i^{\bar{m}} \leq k, \bar{m} = 0, 1, 2, \ldots\big\}. \tag{10}$$

$\delta_i(k)$ is an additional introduced internal dynamical variable of which the initial conditions are considered to be $\delta_i(0) \geq 0$ $\forall i \in \mathcal{N}$.

Lemma 2 [45]: Under the initial state $\delta_i(0) \geq 0 \forall i \in \mathcal{N}$, the internal variable $\delta_i(k)$ of the DDET mechanism given in (8) and (9) satisfies $\delta_i(k) \geq 0$ $\forall k \in \mathbb{Z}_+$ if the selected parameters $\theta_i \in (0, \infty)$ and $\varrho_i \in (0, 1)$ ensure $\theta_i \varrho_i \geq 1$ $\forall i \in \mathcal{N}$.

Remark 4: It can be noted from (10) that, $\forall i \in \mathcal{N}$

$$\bar{\zeta}_i(k) = \begin{cases} 0, & k = k_i^m \text{ or } k = k_i^{m+1} \\ \zeta_i(k), & k \in \left(k_i^m, k_i^{m+1}\right). \end{cases} \tag{11}$$

Taking the event-triggered condition (8) into account, it is not difficult to deduce that $\forall k \in [k_i^m, k_i^{m+1}), m = 0, 1, 2, \ldots$

$$\delta_i(k) + \theta_i\left(\vartheta_i e_i^T(k)e_i(k) - \bar{\zeta}_i^T(k)\bar{\zeta}_i(k)\right) > 0. \tag{12}$$

For the designed scheme [see (8) and (9)], the bigger the triggering interval, the lower the frequency of data transmission, which is conducive to the saving of limited communication resources. To enlarge the triggering interval, a prevailing method is introducing a nonnegative internal dynamic variable, as stated in [42]. In this article, the constraint conditions in Lemma 2 are utilized to ensure the nonnegativity of the variable $\delta_i(k)$. Detailedly, since $\delta_i(0) \geq 0$, we suppose that $\delta_i(k_i^m) \geq 0$. Then, it can be obtained from (9) and (11) that $\delta_i(k_i^m+1) \geq 0$ as $\theta_i \in (0,\infty)$ and $\varrho_i \in (0,1)$. $\forall k \in (k_i^m, k_i^{m+1})$, in terms of (12) and $\theta_i\varrho_i \geq 1$, we can further obtain $\delta_i(k+1) \geq 0$ if $\delta_i(k) \geq 0$. Thus, based on the mathematical induction method, we obtain $\delta_i(k) \geq 0$ $\forall k \in \mathbb{Z}_+$.

Under the above designed DDET mechanism, the control input is considered to be generated by a zero-order holder. Then, the event-triggered equivalent control law for node i can be derived as:

$$u_i(k) = K_i e_i(k_i^m), \quad k \in \left[k_i^m, k_i^{m+1}\right) \tag{13}$$

where $K_i \in \mathbb{R}^{n\times n}$ signifies the controller gain matrix to be designed of node i. Then, synthesizing (6), (7), and (13), the bipartite synchronization error system in the compact form can be derived as follows:

$$\begin{aligned} e(k+1) &= \tilde{A}_{r_1} e(k) - \bar{\Psi}\mathcal{K}\bar{\zeta}(k) \\ &\quad + \tilde{B} f(e(k)) + \tilde{E}\varpi(k) \\ \tilde{z}(k) &= \tilde{F} e(k) \end{aligned} \tag{14}$$

where

$$\begin{aligned} \tilde{x}(k) &\triangleq \begin{bmatrix} \tilde{x}_1^T(k) & \tilde{x}_2^T(k) & \cdots & \tilde{x}_N^T(k) \end{bmatrix}^T \\ \bar{\zeta}(k) &\triangleq \begin{bmatrix} \bar{\zeta}_1^T(k) & \bar{\zeta}_2^T(k) & \cdots & \bar{\zeta}_N^T(k) \end{bmatrix}^T \\ z(k) &\triangleq \begin{bmatrix} z_1^T(k) & z_2^T(k) & \cdots & z_N^T(k) \end{bmatrix}^T \\ \bar{z}(k) &\triangleq \begin{bmatrix} \bar{z}_1^T(k) & \bar{z}_2^T(k) & \cdots & \bar{z}_N^T(k) \end{bmatrix}^T \\ e(k) &\triangleq \tilde{x}(k) - \mathbf{1}_N \otimes s(k), \bar{\Psi} \triangleq \Psi \otimes I_n \\ \tilde{z}(k) &\triangleq z(k) - \mathbf{1}_N \otimes \bar{z}(k), \quad \mathcal{K} \triangleq \mathrm{diag}\{K_1, K_2, \ldots, K_N\} \\ \tilde{A}_{r_1} &\triangleq I_N \otimes A - c(\vec{\mathcal{L}}^{r_1} \otimes I_n) + \bar{\Psi}\mathcal{K}, \quad \tilde{F} \triangleq I_N \otimes F \\ \tilde{B} &\triangleq I_N \otimes B, \quad \tilde{E} \triangleq \bar{\Psi}\begin{bmatrix} E_1^T & E_2^T & \cdots & E_N^T \end{bmatrix}^T \end{aligned}$$

and

$$\begin{aligned} f(e(k)) &\triangleq f(\tilde{x}(k)) - \mathbf{1}_N \otimes f(s(k)), \quad f(\tilde{x}(k)) \\ &\triangleq \begin{bmatrix} f^T(\tilde{x}_1(k)) & f^T(\tilde{x}_2(k)) & \cdots & f^T(\tilde{x}_N(k)) \end{bmatrix}^T. \end{aligned}$$

Definition 3 [18], [47]: Given the gauge transformation matrix $\Psi \triangleq \mathrm{diag}\{\psi_1, \psi_2, \ldots, \psi_N\}$ ($\psi_i \in \{1,-1\}, i \in \mathcal{N}$), the systems (2) and (6) achieve bipartite synchronization in the mean-square sense if $\lim_{k\to\infty} \mathcal{E}\{\|\psi_i x_i(k) - s(k)\|\} = 0$ $\forall i \in \mathcal{N}$.

Remark 5: Suppose that $h_{ij}^{r_1} \geq 0$ $\forall i, j \in \mathcal{N}_1$, and $h_{ij}^{r_1} \leq 0$ $\forall i \in \mathcal{N}_1, j \in \mathcal{N}_2$; then, the bipartite synchronization means

$$\begin{cases} \lim\limits_{k\to\infty} \mathcal{E}\{\|x_i(k) - s(k)\|^2\} = 0 & \forall i \in \mathcal{N}_1 \\ \lim\limits_{k\to\infty} \mathcal{E}\{\|x_i(k) + s(k)\|^2\} = 0 & \forall i \in \mathcal{N}_2. \end{cases}$$

Noteworthy, the switching of the graph only involves the connected weight rather than the cooperation-competition relationships among nodes, which means that the variation of $\eta(k)$ has no effect on the dividing of node set $\mathcal{N}$. Moreover, instead of proving Definition 3 directly, this article will concentrate on proving that the bipartite synchronization error system (14) is mean-square exponentially stable (MSES) [33], i.e.,

$$\mathcal{E}\{\|e(k)\|^2\} \leq \alpha\beta^{k-k_0}\mathcal{E}\{\|e(k_0)\|^2\} \quad \forall k \geq k_0 \tag{15}$$

under the condition of $\omega(l) \equiv 0$. The scalars α and β satisfy $\alpha \in (0,\infty)$ and $\beta \in (0,1)$, respectively.

Definition 4 [33]: The bipartite synchronization error system (14) is MSES with a prescribed $\mathcal{H}_\infty$ performance level λ if system (14) is MSES, and for any $\omega(k) \in l_2[0,\infty)$, there exists $\lambda > 0$ such that, under zero-initial conditions, there holds

$$\sum_{k=0}^{\infty} \mathcal{E}\{\|\tilde{z}(k)\|^2\} \leq \lambda^2 \sum_{k=0}^{\infty} \mathcal{E}\{\|\varpi(k)\|^2\}. \tag{16}$$

III. Main Results

In this section, the attention is focused on discussing the bipartite synchronization control scheme based on a DDET mechanism. The mean-square exponential stability and $\mathcal{H}_\infty$ performance of the bipartite synchronization error system (14) are analyzed in Theorem 1. Then, the concrete form of the designed controller gain is presented in Theorem 2. For brevity, we denote

$$\begin{aligned} \varsigma_1 &\triangleq \min_{r_1\in\mathcal{R}, q_1\in\mathcal{Q}}\{\vec{\lambda}_{\min}(P_{r_1q_1})\}, \quad \bar{\varepsilon} \triangleq \varepsilon^{\left[\frac{1}{(T_P+\tau_P)}+1\right](T_P+1)} \\ \varsigma_2 &\triangleq \max_{r_1\in\mathcal{R}, q_1\in\mathcal{Q}}\{\vec{\lambda}_{\max}(P_{r_1q_1})\}, \quad \bar{\beta} \triangleq \beta\varepsilon^{(T_P+1)/(T_P+\tau_P)} \\ \gamma_M &\triangleq \max_{i\in\mathcal{N}}\{\gamma_i\}, \quad \bar{\delta}(k) \triangleq \left[\, \delta_1^{1/2}(k) \cdots \delta_N^{1/2}(k) \,\right]^T \\ t_k &\triangleq \sup\{g_\upsilon + \kappa \,|\, k_{g_\upsilon+\kappa} \leq k\}, \quad k_{g_1} \triangleq k_0 \\ \Phi_k &\triangleq \tilde{z}^T(k)\tilde{z}(k) - \lambda^2\varpi^T(k)\varpi(k). \end{aligned}$$

A. Stabilization and Performance Analysis

Theorem 1: Construct a candidate Lyapunov function for the bipartite synchronization error system (14) as

$$V_{\eta(k)\sigma(k)}(k) = e^T(k)P_{\eta(k)\sigma(k)}e(k) + \sum_{i=1}^{N}\gamma_i\delta_i(k) \tag{17}$$

where $\delta_i(k)$ developed in (8) and (9) satisfies $\delta_i(0) \geq 0$, $\theta_i > 0$, $0 < \varrho_i < 1$, and $\theta_i\varrho_i \geq 1$ $\forall i \in \mathcal{N}$. For given scalars $0 < \beta < 1$, $\varepsilon > 1$, and $\lambda > 0$, if there exist $\gamma_i > 0 (\forall i \in \mathcal{N})$ and symmetric matrices $P_{r_1q_1} > 0 (\forall r_1 \in \mathcal{R}, q_1 \in \mathcal{Q})$, such that, $\forall \eta(k) \in \mathcal{R}$, $\sigma(k) \in \mathcal{Q}$, the following conditions hold:

$$\mathcal{E}\{V_{\eta(k+1)\sigma(k_{t_k})}(k+1) - \beta V_{\eta(k)\sigma(k)}(k) + \Phi_k\} \leq 0 \tag{18}$$

$$\mathcal{E}\{V_{\eta(k_{g_\upsilon})\sigma(k_{g_\upsilon})}(k_{g_\upsilon}) - \varepsilon V_{\eta(k_{g_\upsilon})\sigma(k_{g_\upsilon}^-)}(k_{g_\upsilon})\} \leq 0 \tag{19}$$

$$\varepsilon^{T_P+1}\beta^{T_P+\tau_P} - 1 < 0. \tag{20}$$

Then, the bipartite synchronization of systems (2) and (6) is achieved, and the prescribed $\mathcal{H}_\infty$ performance index is

$$\bar{\lambda} = \lambda\sqrt{\bar{\varepsilon}(1-\beta)/(1-\bar{\beta})}. \tag{21}$$

Proof: Considering $k \in [k_{g_\upsilon}, k_{g_{\upsilon+1}})$, then, based on conditions (18) and (19), the following inequality can be deduced by recurrence:

$$\begin{aligned}\mathcal{E}\big\{V_{\eta(k)\sigma(k)}(k)\big\} &\le \varepsilon\beta^{k-k_{g_v}}\mathcal{E}\left\{V_{\eta(k_{g_v})\sigma(k_{g_v}^-)}(k_{g_v})+\sum_{l=k_{g_v}}^{k-1}\beta^{k-l-1}\Phi_l\right\}\\ &\le \varepsilon^{\Omega(k_0,k)}\beta^{k-k_0}\mathcal{E}\{V_{\eta(k_0)\sigma(k_0)}(k_0)\}\\ &\quad+\sum_{l=k_0}^{k-1}\varepsilon^{\Omega(l,k)}\beta^{k-l-1}\mathcal{E}\{\Phi_l\}. \end{aligned}\tag{22}$$

Subsequently, we will complete the proof of the theorem from the following two aspects.

Step 1: For $\omega(k)\equiv 0$, we prove the mean-square exponential stability of the bipartite synchronization error system (14).

It is obvious that it can be derived from (17) and Lemma 2 that

$$\varsigma_1\|e(k)\|^2\le V_{\eta(k)\sigma(k)}(k)\le\varsigma_2\|e(k)\|^2+\gamma_M\left\|\bar{\delta}(k)\right\|^2. \tag{23}$$

Under the condition of $\omega(k)\equiv 0$, inequality (22) implies

$$\mathcal{E}\big\{V_{\eta(k)\sigma(k)}(k)\big\}\le\varepsilon^{\left(\frac{k-k_0}{T_P+\tau_P}+1\right)(T_P+1)}\beta^{k-k_0}\mathcal{E}\big\{V_{\eta(k_0)\sigma(k_0)}(k_0)\big\} \tag{24}$$

by taking the constraint (4) about the switching times over $(k_0,k]$ into account. Furthermore, combining (23) with (24) yields

$$\mathcal{E}\{\|e(k)\|^2\}\le\bar{\alpha}\bar{\beta}^{k-k_0}\|e(k_0)\|^2$$

where $\bar{\alpha}\triangleq\varsigma\varepsilon^{T_P+1}/\varsigma_1$ with $\varsigma\triangleq(\varsigma_2\|e(k_0)\|^2+\gamma_M\|\bar{\delta}(k_0)\|^2)/\|e(k_0)\|^2$. Apparently, $\bar{\alpha}>0$ and condition (20) ensure $0<\bar{\beta}<1$. Thus, the synchronization error system (14) is MSES. This combined with Definition 3 means that the bipartite synchronization of $x_i(t)$ and $s(t)$ is achieved at an exponential convergence rate in the mean-square sense.

Step 2: Under zero-initial conditions, we prove the $\mathcal{H}_\infty$ performance of error system (14).

Since $V_{\eta(k)\sigma(k)}(k)\ge 0$, under the conditions of $e(k_0)=0$ and $\bar{\delta}(k_0)=0$, it can be inferred from (22) that

$$\sum_{l=k_0}^{k-1}\varepsilon^{\Omega(l,k)}\beta^{k-l-1}\mathcal{E}\{\Phi_l\}\ge 0$$

which means that

$$\sum_{k=k_0+1}^{\infty}\sum_{l=k_0}^{k-1}\varepsilon^{\Omega(l,k)}\beta^{k-l-1}\mathcal{E}\{\Phi_l\}\ge 0. \tag{25}$$

For inequality (25), by exchanging the summation order and utilizing the equal ratio summation formula, one can deduce that

$$\sum_{k=0}^{\infty}\mathcal{E}\{\|\tilde{z}(k)\|^2\}\le\bar{\lambda}^2\sum_{k=0}^{\infty}\mathcal{E}\{\|\varpi(k)\|^2\}. \tag{26}$$

This completes the proof.

Remark 6: In the construction of the Lyapunov function, not only the double-layer switching signal $\eta(k)$ together with $\sigma(k)$ is taken into consideration but also the internal dynamic nonnegative variable $\delta_i(k)$ corresponding to the triggering scheme is considered. Furthermore, the variation of the Lyapunov function is considered to have different trends at the switching and nonswitching instants of the PDT switching signal, as shown in (18) and (19). The synthesis of the switching and triggering features to (17) may make the established Lyapunov function more comprehensive, which is conducive to deriving conditions with less conservatism.

Remark 7: For networks with antagonistic interactions, many prominent results about bipartite consensus under structural balance or stability under structural unbalance have emerged in recent years [15], [48], [49]. It can be noted that these results mainly focus on investigating $\lim_{k\to\infty}|x_i(k)|=c$, where structurally balanced case induces $c\neq 0$ corresponding to bipartite consensus and structurally unbalanced case derives $c=0$ corresponding to stability. Different from these studies, this article is interested in achieving $\lim_{k\to\infty}\mathcal{E}\{\|\psi_i x_i(k)-s(k)\|\}=0$, i.e., enforcing the dynamics of networks converging to a specified trajectory $s(k)$ or the opposite of $s(k)$ by virtue of the DDET control scheme. Since the dynamic of $s(k)$ can be stable, oscillating, chaotic, or even diverging, under structurally unbalanced cases, it may be infeasible to bipartite synchronize the dynamics of nodes to the special value 0 as in [49]. Therefore, our attention mainly centers on the simultaneously structurally balanced signed graph.

B. Event-Triggered Controller Design

Theorem 2: Assume that the internal variable $\delta_i(k)$ of the event-triggered scheme (8) and (9) satisfies $\delta_i(0)\ge 0$, and the scalars $\theta_i>0$ and $0<\varrho_i<1$ meet $\theta_i\varrho_i\ge 1$ $\forall i\in\mathcal{N}$. Given constants $0<\beta<1$, $\varepsilon>1$, and $\lambda>0$, if there exist $\gamma_i>0$ and $\mu^i_{r_1q_1}>0(\forall i\in\mathcal{N})$, symmetric matrix $P_{r_1q_1}>0$, diagonal matrix $\Lambda_{r_1q_1}>0$, $\bar{\mathcal{K}}$, and invertible diagonal matrix J, such that, $\forall r_1\in\mathcal{R}$, $q_1\in\mathcal{Q}$, inequality (20) and the following inequalities hold

$$\Xi_{r_1q_1}\triangleq\begin{bmatrix}\varphi^{11}_{r_1q_1} & 0 & \Lambda_{r_1q_1}F_2 & 0 & \varphi^{15}_{r_1q_1}\\ * & \varphi^{22}_{r_1q_1} & 0 & 0 & \varphi^{25}_{r_1q_1}\\ * & * & -\Lambda_{r_1q_1} & 0 & \varphi^{35}_{r_1q_1}\\ * & * & * & \varphi^{44}_{r_1q_1} & \varphi^{45}_{r_1q_1}\\ * & * & * & * & \varphi^{55}_{q_1}\end{bmatrix}<0 \tag{27}$$

$$P_{r_1q_1}-\varepsilon P_{r_1q_2}<0,\quad q_1\neq q_2,\ q_1,\ q_2\in\mathcal{Q} \tag{28}$$

where

$$\begin{aligned}\varphi^{11}_{r_1q_1}&\triangleq\Upsilon\hat{\vartheta}+\tilde{F}^T\tilde{F}-\beta P_{r_1q_1}+\Gamma_{r_1q_1}\hat{\theta}-\Lambda_{r_1q_1}F_1\\ \Pi^{q_1}_{r_1}&\triangleq\left[\sqrt{\bar{\pi}^{q_1}_{r_11}}I_{Nn}\quad\sqrt{\bar{\pi}^{q_1}_{r_12}}I_{Nn}\quad\cdots\quad\sqrt{\bar{\pi}^{q_1}_{r_1R}}I_{Nn}\right]\\ \varphi^{15}_{r_1q_1}&\triangleq\left[(I_N\otimes A^T-c(\vec{\mathcal{L}}^{r_1}\otimes I_n)^T)J^T+\bar{\Psi}\bar{\mathcal{K}}^T\right]\Pi^{q_1}_{r_1}\\ \varphi^{22}_{r_1q_1}&\triangleq-\Upsilon-\Gamma_{r_1q_1}\check{\theta},\quad\varphi^{25}_{r_1q_1}\triangleq-\bar{\Psi}\bar{\mathcal{K}}^T\Pi^{q_1}_{r_1}\\ \varphi^{35}_{r_1q_1}&\triangleq\tilde{B}^TJ^T\Pi^{q_1}_{r_1},\quad\varphi^{45}_{r_1q_1}\triangleq\begin{bmatrix}0 & \Pi^{q_1T}_{r_1}J\tilde{E}\end{bmatrix}^T\\ \varphi^{44}_{r_1q_1}&\triangleq\mathrm{diag}\{\bar{\Upsilon}\bar{\varrho}-\beta\bar{\Upsilon}+\bar{\Gamma}_{r_1q_1},-\lambda^2I_{n_\varpi}\}\\ \varphi^{55}_{q_1}&\triangleq\mathrm{diag}\{P_{1q_1}-\mathrm{sym}(J),\ldots,P_{Rq_1}-\mathrm{sym}(J)\}\end{aligned}$$

with

$$\begin{aligned}
\bar{\Upsilon} &\triangleq \mathrm{diag}\{\gamma_1,\ldots,\gamma_N\},\quad \Upsilon \triangleq \bar{\Upsilon}\otimes I_n\\
\bar{\Gamma}_{r_1q_1} &\triangleq \mathrm{diag}\{\mu^1_{r_1q_1},\ldots,\mu^N_{r_1q_1}\},\quad \Gamma_{r_1q_1}\triangleq \bar{\Gamma}_{r_1q_1}\otimes I_n\\
\bar{\vartheta} &\triangleq \mathrm{diag}\{\vartheta_1,\ldots,\vartheta_N\},\quad \bar{\theta}\triangleq \mathrm{diag}\{\theta_1,\ldots,\theta_N\}\\
\bar{\varrho} &\triangleq \mathrm{diag}\{\varrho_1,\ldots,\varrho_N\},\quad \hat{\vartheta}\triangleq \bar{\vartheta}\otimes I_n, \check{\theta}\triangleq \bar{\theta}\otimes I_n\\
F_1 &\triangleq I_N\otimes \mathrm{diag}\{\tau_1^-\tau_1^+,\ldots,\tau_n^-\tau_n^+\},\quad \hat{\theta}\triangleq\check{\theta}\hat{\vartheta}\\
F_2 &\triangleq I_N\otimes \mathrm{diag}\{(\tau_1^-+\tau_1^+)/2,\ldots,(\tau_n^-+\tau_n^+)/2\}.
\end{aligned}$$

Then, systems (2) and (6) achieve bipartite synchronization with a prescribed $\mathcal{H}_\infty$ performance index $\bar{\lambda}$, and the desired controller gain matrix is given by

$$\mathcal{K} = J^{-1}\bar{\mathcal{K}}. \tag{29}$$

Proof: Inspired by Liu *et al.* [50], one can infer from Assumption 2 that

$$\begin{bmatrix} e(k)\\ f(e(k))\end{bmatrix}^T \begin{bmatrix} -\Lambda_{r_1q_1}F_1 & \Lambda_{r_1q_1}F_2\\ * & -\Lambda_{r_1q_1}\end{bmatrix}\begin{bmatrix} e(k)\\ f(e(k))\end{bmatrix}\ge 0. \tag{30}$$

Furthermore, according to the DDET mechanism (8) and (9) and the analysis in Remark 4, it holds that

$$\mu^i_{r_1q_1}\left(\delta_i(k)+\theta_i\left(\vartheta_i e_i^T(k)e_i(k)-\bar{\zeta}_i^T(k)\bar{\zeta}_i(k)\right)\right) > 0 \tag{31}$$

$\forall k\ge k_0, \mu^i_{r_1q_1} > 0$. Then, by synthesizing the situation of N nodes, we obtain

$$\bar{\delta}^T(k)\bar{\Gamma}_{r_1q_1}\bar{\delta}(k)+e^T(k)\Gamma_{r_1q_1}\hat{\theta}e(k)-\bar{\zeta}^T(k)\Gamma_{r_1q_1}\check{\theta}\bar{\zeta}(k)\ge 0. \tag{32}$$

In addition, with regard to inequality (27), apply inequality $-JP^{-1}_{\tilde{r}q_1}J^T \le P_{\tilde{r}q_1}-\mathrm{sym}(J)$, equality $\bar{\mathcal{K}} = J\mathcal{K}$, and congruent transformation (with the corresponding matrix being $\bar{\mathcal{J}} = \mathrm{diag}\{I,I,I,I,I_R\otimes J^{-1}\}$) to it. Then, for the obtained inequality, utilizing the Schur complement straightforwardly deduces

$$\begin{aligned}
&\mathcal{E}\{V_{\eta(k+1)q_1}(k+1)-\beta V_{\eta(k)q_1}(k)+\Phi_k\}\\
&\quad=\sum_{\tilde{r}=1}^{R}\tilde{\pi}^{q_1}_{r_1\tilde{r}}e^T(k+1)P_{\tilde{r}q_1}e(k+1)+\Phi_k+\sum_{i=1}^{N}\gamma_i\\
&\qquad\times\delta_i(k+1)-\beta\left(e^T(k)P_{r_1q_1}e(k)+\sum_{i=1}^{N}\gamma_i\delta_i(k)\right)\\
&\quad\le\tilde{\xi}^T(k)\tilde{\Xi}_{r_1q_1}\tilde{\xi}(k)\\
&\quad\le 0
\end{aligned}\tag{33}$$

based on (14) and (17), where

$$\begin{aligned}
\tilde{\xi}^T(k) &\triangleq \begin{bmatrix} e^T(k) & \bar{\zeta}^T(k) & f^T(e(k)) & \bar{\delta}^T(k) & \varpi^T(k)\end{bmatrix}\\
\tilde{\Xi}_{r_1q_1} &\triangleq \begin{bmatrix} \tilde{\varphi}^{11}_{r_1q_1} & 0 & \tilde{\varphi}^{13}_{r_1}\\ * & \bar{\Upsilon}\bar{\varrho}-\beta\bar{\Upsilon}+\bar{\Gamma}_{r_1q_1} & 0\\ * & * & \hat{\varphi}_{(\tilde{E},\tilde{E})}-\lambda^2 I\end{bmatrix}\\
\tilde{\varphi}^{11}_{r_1q_1} &\triangleq \begin{bmatrix} \check{\varphi}^{11}_{r_1q_1} & -\hat{\varphi}_{(\tilde{A}_{r_1},\bar{\Psi}\mathcal{K})} & \hat{\varphi}_{(\tilde{A}_{r_1},\tilde{B})}+\Lambda_{r_1q_1}F_2\\ * & \check{\varphi}^{22}_{r_1q_1} & -\hat{\varphi}_{(\bar{\Psi}\mathcal{K},\tilde{B})}\\ * & * & \hat{\varphi}_{(\tilde{B},\tilde{B})}-\Lambda_{r_1q_1}\end{bmatrix}\\
\check{\varphi}^{11}_{r_1q_1} &\triangleq \hat{\varphi}_{(\tilde{A}_{r_1},\tilde{A}_{r_1})}+\varphi^{11}_{r_1q_1},\quad \check{\varphi}^{22}_{r_1q_1}\triangleq\hat{\varphi}_{(\bar{\Psi}\mathcal{K},\bar{\Psi}\mathcal{K})}+\varphi^{22}_{r_1q_1}\\
\tilde{\varphi}^{13}_{r_1} &\triangleq \begin{bmatrix}\hat{\varphi}^T_{(\tilde{A}_{r_1},\tilde{E})} & -\hat{\varphi}^T_{(\bar{\Psi}\mathcal{K},\tilde{E})} & \hat{\varphi}^T_{(\tilde{B},\tilde{E})}\end{bmatrix}^T
\end{aligned}$$

with $\hat{\varphi}_{(\hat{U},\hat{V})}\triangleq\sum_{\tilde{r}=1}^{R}\tilde{\pi}^{q_1}_{r_1\tilde{r}}\hat{U}^TP_{\tilde{r}q_1}\hat{V}$. Thus, condition (18) holds. Moreover, condition (28) ensures

$$\mathcal{E}\{V_{\eta(k_{g_v})q_1}(k_{g_v})-\varepsilon V_{\eta(k_{g_v})q_2}(k_{g_v})\}\le 0 \tag{34}$$

$\forall q_1\ne q_2, q_1,q_2\in\mathcal{Q}$, which means that (19) is satisfied.

Remark 8: For the event-triggered mechanism, there exists a crucial issue in the processing process, i.e., how to introduce the relevant restrictions on triggering conditions into the analysis of the Lyapunov function. Thus, the positive internal variable $\delta_i(k)$ is constructed in the Lyapunov function. Moreover, since the input of the controller is updated only when the triggering conditions in (8) and (9) are satisfied, with the employ of the specially defined variable $\bar{\zeta}_i(k)$, inequality (31) holds for $\forall k\ge k_0$. Besides, for the weighted signed graph $\mathcal{G}^{r_1}$ containing cooperation-competition interactions, $\bar{\Psi}$ is employed for matrix transformation. During the treatment process of inequality (33), there exists coupling term $J\bar{\Psi}\mathcal{K}$ (J and $\mathcal{K}$ are unknown), which makes the calculation of the gain matrix $\mathcal{K}$ intractable by using a solver based on linear matrix inequalities. Therefore, considering the block diagonal property of the matrix $\mathcal{K}$ and the specific form of the gauge transformation matrix $\bar{\Psi}$, the transformation $\mathcal{K}\bar{\Psi}=\bar{\Psi}\mathcal{K}$ is performed. Then, we define $J\mathcal{K}$ as $\bar{\mathcal{K}}$. On this account, the matrix inequality no longer contains the coupling term constituting of unknown matrices.

IV. Illustrative Examples

In this section, we employ two numerical examples of NNs with cooperation-competition interactions and double-layer switching topologies to verify the effectiveness of the designed DDET $\mathcal{H}_\infty$ controller. The first example considers the bipartite synchronization issue of chaotic NNs. The second example analyzes the advantages of the DDET transmission mechanism in saving communication bandwidth compared with a traditional static one.

Example 1: The chaotic NNs considered here have four nodes, and each node contains three neurons. The switching topologies $\mathcal{G}^1$ and $\mathcal{G}^2$ are presented in Fig. 2, of which the node set can be divided as $\mathcal{N}_1=\{1,4\}$ and $\mathcal{N}_2=\{2,3\}$, according to Definition 1. Then, the Laplacian matrices are

$$\mathcal{L}^1=\begin{bmatrix}0.2 & 0 & 0 & -0.2\\ 0.3 & 0.6 & 0 & 0.3\\ 0 & -0.4 & 0.4 & 0\\ 0 & 0 & 0.2 & 0.2\end{bmatrix}$$
$$\mathcal{L}^2=\begin{bmatrix}0.2 & 0 & 0 & -0.2\\ 0.3 & 0.3 & 0 & 0\\ 0.1 & -0.4 & 0.5 & 0\\ 0 & 0 & 0.2 & 0.2\end{bmatrix}.$$

Correspondingly, the gauge transformation matrix Ψ can be selected as $\Psi=\mathrm{diag}\{-1,1,1,-1\}$. The switching of the topologies is considered to be governed by the double-layer switching signal $\eta(k)$, whose parameters are given as follows:

$$\hat{\Lambda}^1=\begin{bmatrix}0.65 & 0.35\\ 0.15 & 0.85\end{bmatrix},\quad \hat{\Lambda}^2=\begin{bmatrix}0.42 & 0.58\\ 0.33 & 0.67\end{bmatrix}$$
$$\tau_P=6,\quad T_P=8,\ \beta=0.9999,\ \varepsilon=1.0001$$

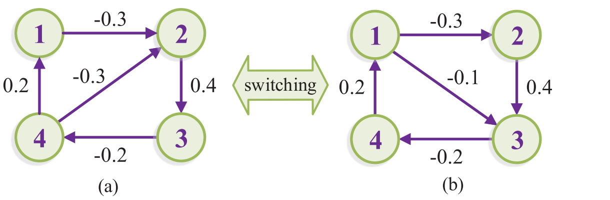

Fig. 2. Switching topologies $\mathcal{G}^1$ and $\mathcal{G}^2$. (a) Signed graph $\mathcal{G}^1$. (b) Signed graph $\mathcal{G}^2$.

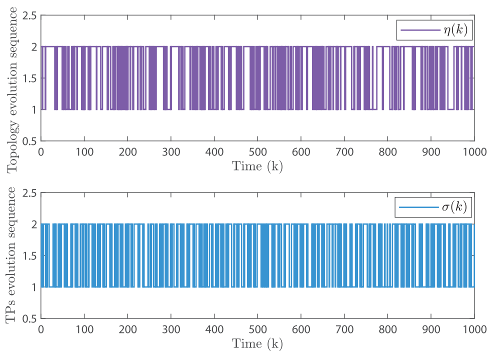

Fig. 3. Possible evolution sequence of the topology switching $\eta(k)$ and TPs switching $\sigma(k)$.

based on which, a set of possible evolution sequences of the topology switching can be obtained, as shown in Fig. 3.

Moreover, the system parameters of each node given by (2) are with the form of

$$A = \mathrm{diag}\{0.9712, 0.9712, 0.9712\}, \quad c = 1$$
$$B = \begin{bmatrix} 0.0500 & -0.0300 & 0.0125 \\ 0.0625 & 0.0425 & 0.0287 \\ -0.2225 & 0 & -0.0113 \end{bmatrix}$$
$$F = \begin{bmatrix} 0.02 & 0.04 & 0 \\ 0 & 0.04 & 0.06 \\ 0.02 & 0 & 0.04 \end{bmatrix}, \quad E_i = \begin{bmatrix} 0.2 \\ 0.4 \\ 0.7 \end{bmatrix}$$

where $i = 1, 2, 3, 4$. The activation function is chosen as $f(x(k)) = \tanh(x(k))$, which is obviously an odd function satisfying Assumption 2 with the bound being $\tau_\iota^- = 0$ and $\tau_\iota^+ = 1$, $\iota = 1, 2, 3$. The prescribed scalar λ is taken as 0.5, and the external disturbance is taken as $\varpi(k) = 2\exp(-0.1k)\sin(0.2k)$.

Besides, for the DDET mechanism, the following parameters satisfying Lemma 2 are considered:

$$\bar{\vartheta} = \mathrm{diag}\{0.4, 0.5, 0.6, 0.8\}$$
$$\bar{\theta} = \mathrm{diag}\{1.5, 1.7, 1.3, 1.9\}$$
$$\bar{\varrho} = \mathrm{diag}\{0.7, 0.6, 0.8, 0.6\}.$$

Then, by virtue of Theorem 2, the controller gain matrices under the DDET mechanism can be calculated as:

$$K_1 = \mathrm{diag}\{0.8051, 0.8392, 0.8878\}$$
$$K_2 = \mathrm{diag}\{-0.3649, -0.2856, -0.4293\}$$
$$K_3 = \mathrm{diag}\{-0.3089, -0.2722, -0.4651\}$$
$$K_4 = \mathrm{diag}\{0.1757, 0.3341, 0.5074\}.$$

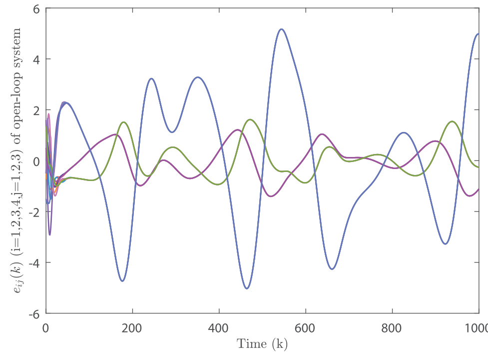

Fig. 4. Bipartite synchronization errors of the open-loop system.

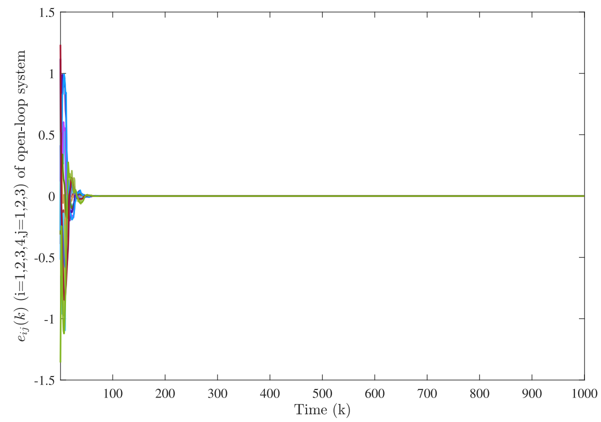

Fig. 5. Bipartite synchronization errors of the closed-loop system.

Remark 9: For the constraint conditions in Theorem 2, we expect to find a set of feasible $\gamma^i_{r_1q_1} > 0$, $\mu^i_{r_1q_1} > 0$, $P_{r_1q_1} > 0$, $\Lambda_{r_1q_1} > 0$, and $\bar{\mathcal{K}}$ and J ($\forall i \in \mathcal{N}$, $r_1 \in \mathcal{R}$, $q_1, q_2 \in \mathcal{Q}$, and $q_1 \neq q_2$), such that conditions (20), (27), and (28) hold. Then, the calculating of the desired controller gain can be transformed to solving the following convex optimization problem:

$$\begin{cases} \min\ t \\ \text{s.t.}\ -\gamma^i_{r_1q_1} < t, -\mu^i_{r_1q_1} < t, -P_{r_1q_1} < -tI \\ -\Lambda_{r_1q_1} < -tI, \varepsilon^{T_P+1}\beta^{T_P+\tau_P} - 1 < t,\ \Xi_{r_1q_1} < -tI \\ P_{r_1q_1} - \varepsilon P_{r_1q_2} < 0 \quad (\forall i \in \mathcal{N}, r_1 \in \mathcal{R}, q_1, q_2 \in \mathcal{Q}, q_1 \neq q_2). \end{cases}$$

If the minimum value of t is negative, it means that constraints in Theorem 2 are satisfied. Then, based on the derived solutions $\bar{\mathcal{K}}$ and J, the desired controller gain matrix $\mathcal{K}$ can be calculated from (29).

The nonnegative initial states of the internal variable $\delta_i(k)$ are selected as $\delta_1(0) = 0.3$, $\delta_2(0) = 0.2$, $\delta_3(0) = 0.5$, and $\delta_4(0) = 0.4$. The initial values of NNs and the isolated node are chosen as $x_1(0) = [0.5; -0.5; -1.6]$, $x_2(0) = [1.2; -1.5; 0]$, $x_3(0) = [-0.5; 0.6; -0.5]$, $x_4(0) = [-0.5; -0.6; 1.5]$, and $s(0) = [0; -0.76; 0]$, respectively. Then, by virtue of Algorithm 1, the simulation results based on the designed controller gains and the switching sequence given in Fig. 3 are illustrated in Figs. 4–8. Specifically, the bipartite synchronization errors of the open- and closed-loop systems are presented in Figs. 4 and 5, respectively. The state

Algorithm 1 Updating of $u(k)$ Under DDET Mechanism

Input: $N, Tall, \delta_i(1), SN_i(1), Ee_i, i \in \mathcal{N}, \bar{\vartheta}, \bar{\theta}, \bar{\varrho}$;
Output: Controller output: $u(k)$.

Determine Ψ according to the graph;
Compute $K_i, i \in \mathcal{N}$ based on Theorem 2;
Load the switching sequence $\eta(k)$ of the topology;
for $k = 1 : Tall$ **do**
  for $i = 1 : N$ **do**
    $\zeta_i(k) = e_i(k) - Ee_i$;
    if $\delta_i(k) + \theta_i(\vartheta_i e_i^T(k)e_i(k) - \zeta_i^T(k)\zeta_i(k)) \le 0$ **then**
      $Ee_i = e_i(k)$;
    else
      $\bar{\zeta}_i(k) = e_i(k) - Ee_i$;
      $\delta_i(k+1) = \varrho_i\delta_i(k) + \vartheta_i e_i^T(k)e_i(k) - \bar{\zeta}_i^T(k)\bar{\zeta}_i(k)$;
  $Ee(k) = (Ee_1; Ee_2 \ldots; Ee_N)$;
  Calculate $u(k) = \mathcal{K}Ee(k)$;
  Update $e_i(k), s(k)$ based on (6) and (14).

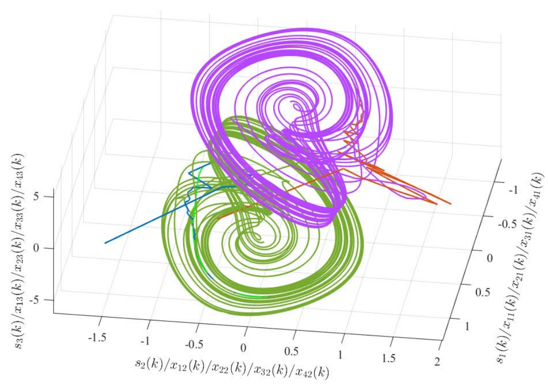

Fig. 6. State trajectories of the isolated node and the network nodes.

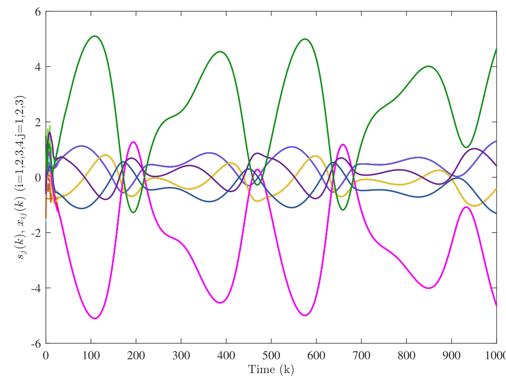

Fig. 7. State responses of the isolated node and the network nodes.

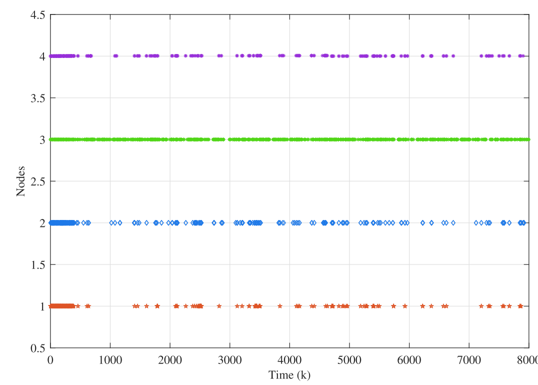

Fig. 8. Updating instants of the controller input under the DDET mechanism.

trajectories and responses of the isolated node and the network nodes with control input are presented in Figs. 6 and 7. Moreover, the updating instants of the controller input under the event-triggered mechanism are given in Fig. 8. It should be mentioned that the total interval length under consideration is $[0, 8000]$. However, for the purpose of clearer observation, some figures are presented with the interval length $[0, 1000]$. It is obvious that, with the designed DDET controller, the error states converge to zero eventually, which means that the bipartite synchronization of the isolated node and the network nodes is achieved. Furthermore, the triggering rates (TRs) of the four nodes are 4.2750%, 4.8000%, 12.4875%, and 3.6875%, respectively, which indicates that the frequency transmission has been reduced effectively.

Example 2: Consider the cooperation-competition NNs with switching topologies $\mathcal{G}^1$ and $\mathcal{G}^2$ shown in Fig. 2, of which the dividing of node set and the selection of matrix Ψ are the same as the ones in Example 1. Moreover, the switching of the topologies is considered to be governed by the sequence presented in Fig. 3. Taking the following system parameters into consideration:

$$A = \mathrm{diag}\{0.95, 0.95, 0.95, 0.95\}, \quad c = 1, \ \lambda = 8.5$$

$$B = \begin{bmatrix} 0.0425 & -0.1000 & -0.0250 & 0.0250 \\ 0.0900 & 0.0575 & 0.0300 & 0.0150 \\ 0.0550 & 0.0605 & 0.1250 & 0.0025 \\ 0.0050 & -0.0200 & -0.0750 & 0.0725 \end{bmatrix}$$

$$F = \begin{bmatrix} 0.15 & 0.04 & 0.13 & 0.3 \\ 0.01 & 0.25 & 0.03 & 0.21 \\ 0.04 & 0.22 & 0.02 & 0.05 \end{bmatrix}, \quad E = \begin{bmatrix} 0.3 \\ 0.5 \\ 0.4 \\ 0.6 \end{bmatrix}.$$

The activation function, the external disturbance, and the event-triggered relevant parameters are taken the same forms as the ones in Example 1. Then, the following controller gains can be obtained based on Theorem 2:

$$K_1 = \mathrm{diag}\{0.7283, 0.8601, 0.9472, 0.7968\}$$
$$K_2 = \mathrm{diag}\{-0.3639, -0.3878, -0.5353, -0.4209\}$$
$$K_3 = \mathrm{diag}\{-0.4018, -0.3999, -0.5262, -0.5020\}$$
$$K_4 = \mathrm{diag}\{0.4298, 0.4634, 0.6088, 0.5111\}.$$

Consider the total time interval being $[0, 2000]$, and the initial states are selected as $s(0) = [0.15; 0.2; -0.3; -0.2]$, $x_1(0) = [0.1; 0.1; 0.1; 0.2]$, $x_2(0) = [-0.2; 0.2; -0.2; -0.4]$, $x_3(0) = [0.1; 0.1; 0.1; 0.2]$, and $x_4(0) = [-0.3; -0.2; 0.5; 0.4]$. Then, the bipartite synchronization errors of the open-loop system and the state

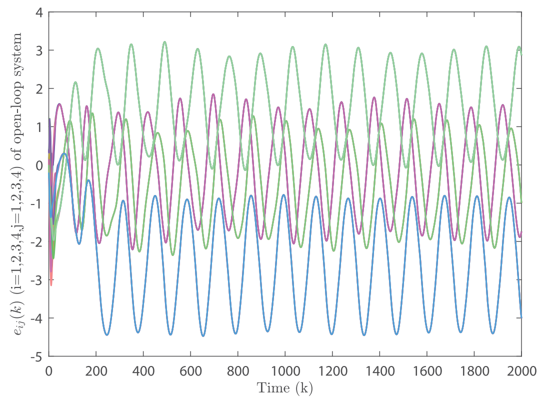

Fig. 9. Bipartite synchronization errors of the open-loop system.

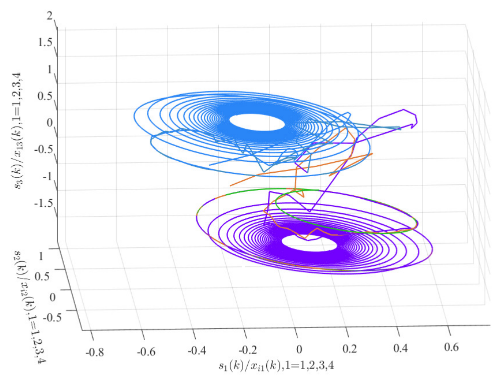

Fig. 10. State trajectories of the isolated node and the neural network (a).

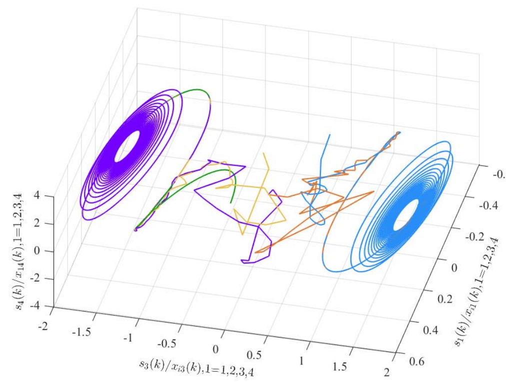

Fig. 11. State trajectories of the isolated node and the neural network (b).

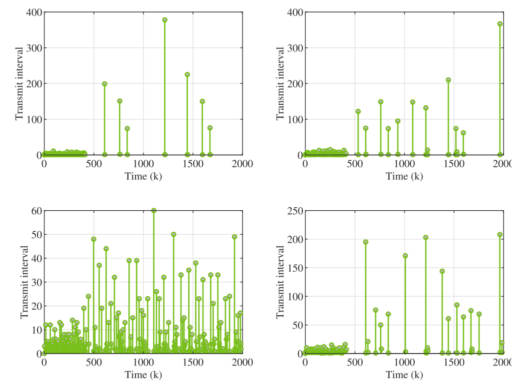

Fig. 12. Triggering intervals.

trajectories of the isolated node and the neural network are presented in Figs. 9–11, respectively. It can be seen that the open-loop neural network cannot reach the desired bipartite synchronization, while the closed-loop system does so. Moreover, the triggering intervals are plotted in Fig. 12, which shows the effectiveness of the event-triggered scheme. Under zero-initial conditions, the actual $\mathcal{H}_\infty$ performance can be examined as:

$$\sqrt{\frac{\sum_{l=0}^{2000}\mathcal{E}\{\tilde{z}^T(l)\tilde{z}(l)\}}{\sum_{l=0}^{2000}\mathcal{E}\{\omega^T(l)\omega(l)\}}} = 1.0932 < \bar{\lambda} = 14.2286$$

which means that the performance index is within the prescribed value. It should be mentioned that the calculated actual $\mathcal{H}_\infty$ performance is much smaller than the prescribed value $\bar{\lambda}$. This is mainly caused by the conservatism of the derived conditions. Therefore, the adopted method still needs to be improved.

Furthermore, if the internal variables $\delta_i(k)(i \in \mathcal{N})$ are considered to be zero, the DDET condition will degrade into a static one as

$$k_i^{m+1} = \inf\left\{k \in \mathbb{Z}_+ \middle| k > k_i^m,\ \vartheta_i\|e_i(k)\|_2^2 - \|\zeta_i(k)\|_2^2 \le 0\right\}.$$

Then, for the interval [0, 500], the TRs of nodes 1–4 under the DDET scheme and static one are calculated in Table I. Evidently, the dynamic event-triggered mechanism has notable superiority in reducing the transmission frequency.

Besides, for simplicity, we choose $\theta_i = \theta$ for $i \in \mathcal{N}$. In order to investigate the relationship among the triggering scalar θ, the sampling instant variation rate β, and the system performance, the optimal performance index $\bar{\lambda}_{\min}$ corresponding to different pairs (θ, β) is presented in Table II. It indicates that selecting a suitable pair of (θ, β) may be beneficial to obtain a better performance index of the system.

TABLE I
TRs of Nodes 1–4 Under the DDET Scheme and Static One

TRs	Node 1	Node 2	Node 3	Node 4	Average
Dynamic	35.8%	27.4%	21.8%	22.4%	26.85%
Static	56.0%	59.0%	46.6%	45.8%	51.85%

TABLE II
Optimal Performance Index $\bar{\lambda}_{\min}$ for Different Pairs (θ, β)

$\bar{\lambda}_{\min}$	$\beta = 0.99$	$\beta = 0.98$	$\beta = 0.97$	$\beta = 0.96$
$\theta = 2$	4.0179	4.4584	5.1502	6.4809
$\theta = 16$	4.0182	4.4609	5.1672	6.4893
$\theta = 30$	4.0183	4.4615	5.1613	6.4965

V. Conclusion

In this article, the bipartite $\mathcal{H}_\infty$ synchronization issue has been addressed for a class of discrete-time cooperation-competition coupled neural networks with switching topologies and constrained communication bandwidth. The stochastic switching of network topologies has been supposed to be governed by a double-layer switching signal, of which the essential switching framework is a Markov chain with persistent dwell-time switched transition probabilities. In consideration of the limited transmission bandwidth and the complicated structure of neural networks, the distributed dynamic event-triggered mechanism that requires only aperiodic intermittent communication between network and controller has been employed to further reduce the transmission frequency. With the help of the algebraic graph theory, the stochastic theory, and the Lyapunov function method, an event-triggered $\mathcal{H}_\infty$ controller that ensures that the bipartite synchronization of networks can be reached exponentially in the mean-square sense has been constructed. Finally, simulation results, including the investigation of chaotic synchronization behavior and the comparison of distributed dynamic event-triggered mechanism with traditional static one, have been given to illustrate the validity of the proposed control scheme. From a practical perspective, taking the network-induced time delays into consideration in the designing process of dynamic event-triggered control scheme for double-layer switched systems deserves further exploration. Moreover, extending our results to switched networks with both simultaneously structurally balanced and unbalanced topologies by other synchronization/consensus protocols will be also one of our future research directions.

References

[1] H. Sang and J. Zhao, "Sampled-data-based H_∞ synchronization of switched coupled neural networks," *IEEE Trans. Cybern.*, vol. 51, no. 4, pp. 1968–1980, Apr. 2021.

[2] H. Rao, F. Liu, H. Peng, Y. Xu, and R. Lu, "Observer-based impulsive synchronization for neural networks with uncertain exchanging information," *IEEE Trans. Neural Netw. Learn. Syst.*, vol. 31, no. 10, pp. 3777–3787, Oct. 2020.

[3] H. Sang and J. Zhao, "Exponential synchronization and L_2-gain analysis of delayed chaotic neural networks via intermittent control with actuator saturation," *IEEE Trans. Netw. Learn. Syst.*, vol. 30, no. 12, pp. 3722–3734, Dec. 2019.

[4] S. Arik, "New criteria for stability of neutral-type neural networks with multiple time delays," *IEEE Trans. Netw. Learn. Syst.*, vol. 31, no. 5, pp. 1504–1513, May 2020.

[5] Y.-W. Wang, T. Bian, J.-W. Xiao, and C. Wen, "Global synchronization of complex dynamical networks through digital communication with limited data rate," *IEEE Trans. Neural Netw. Learn. Syst.*, vol. 26, no. 10, pp. 2487–2499, Oct. 2015.

[6] J. J. de Rubio, "Stability analysis of the modified Levenberg-Marquardt algorithm for the artificial neural network training," *IEEE Trans. Neural Netw. Learn. Syst.*, early access, Aug. 18, 2020, doi: 10.1109/TNNLS.2020.3015200.

[7] T. Huang, C. Li, S. Duan, and J. A. Starzyk, "Robust exponential stability of uncertain delayed neural networks with stochastic perturbation and impulse effects," *IEEE Trans. Neural Netw. Learn. Syst.*, vol. 23, no. 6, pp. 866–875, Jun. 2012.

[8] C. Li and X. Liao, "Robust stability and robust periodicity of delayed recurrent neural networks with noise disturbance," *IEEE Trans. Circuits Syst. I, Reg. Papers*, vol. 53, no. 10, pp. 2265–2273, Oct. 2006.

[9] Y.-J. Liu, C. L. P. Chen, G.-X. Wen, and S. Tong, "Adaptive neural output feedback tracking control for a class of uncertain discrete-time nonlinear systems," *IEEE Trans. Neural Netw.*, vol. 22, no. 7, pp. 1162–1167, Jul. 2011.

[10] H. Zhang, Y. Luo, and D. Liu, "Neural-network-based near-optimal control for a class of discrete-time affine nonlinear systems with control constraints," *IEEE Trans. Neural Netw.*, vol. 20, no. 9, pp. 1490–1503, Sep. 2009.

[11] S. Lakshmanan, M. Prakash, C. P. Lim, R. Rakkiyappan, P. Balasubramaniam, and S. Nahavandi, "Synchronization of an inertial neural network with time-varying delays and its application to secure communication," *IEEE Trans. Neural Netw. Learn. Syst.*, vol. 29, no. 1, pp. 195–207, Jan. 2018.

[12] R. Tang, X. Yang, and X. Wan, "Finite-time cluster synchronization for a class of fuzzy cellular neural networks via non-chattering quantized controllers," *Neural Netw.*, vol. 113, pp. 79–90, May 2019.

[13] C. Chen, L. Li, H. Peng, and Y. Yang, "Fixed-time synchronization of memristor-based BAM neural networks with time-varying discrete delay," *Neural Netw.*, vol. 96, pp. 47–54, Dec. 2017.

[14] S. Chen, H. Jiang, B. Lu, Z. Yu, and L. Li, "Pinning bipartite synchronization for inertial coupled delayed neural networks with signed digraph via non-reduced order method," *Neural Netw.*, vol. 129, pp. 392–402, Sep. 2020.

[15] J. Lu, Y. Wang, X. Shi, and J. Cao, "Finite-time bipartite consensus for multiagent systems under detail-balanced antagonistic interactions," *IEEE Trans. Syst., Man, Cybern. Syst.*, vol. 51, no. 6, pp. 3867–3875, Jun. 2021, doi: 10.1109/TSMC.2019.2938419.

[16] S. Zhai and Q. Li, "Bipartite synchronization in a network of nonlinear systems: A contraction approach," *J. Franklin Inst.*, vol. 353, no. 17, pp. 4602–4619, Nov. 2016.

[17] D. Meng, J. Liang, Y. Wu, and Z. Meng, "Connection of signed and unsigned networks based on solving linear dynamic systems," *IEEE Trans. Syst., Man, Cybern. Syst.*, early access, Oct. 31, 2019, doi: 10.1109/TSMC.2019.2945538.

[18] C. Altafini, "Consensus problems on networks with antagonistic interactions," *IEEE Trans. Autom. Control*, vol. 58, no. 4, pp. 935–946, Apr. 2013.

[19] M. E. Valcher and P. Misra, "On the consensus and bipartite consensus in high-order multi-agent dynamical systems with antagonistic interactions," *Syst. Control Lett.*, vol. 66, pp. 94–103, Apr. 2014.

[20] F. Adib Yaghmaie, R. Su, F. L. Lewis, and S. Olaru, "Bipartite and cooperative output synchronizations of linear heterogeneous agents: A unified framework," *Automatica*, vol. 80, pp. 172–176, Jun. 2017.

[21] J. Qin, W. Fu, W. X. Zheng, and H. Gao, "On the bipartite consensus for generic linear multiagent systems with input saturation," *IEEE Trans. Cybern.*, vol. 47, no. 8, pp. 1948–1958, Aug. 2017.

[22] H.-X. Hu, G. Wen, and W. X. Zheng, "Collective behavior of heterogeneous agents in uncertain cooperation–competition networks: A Nussbaum-type function based approach," *IEEE Trans. Control Netw. Syst.*, vol. 7, no. 2, pp. 783–796, Jun. 2020.

[23] D. Meng, M. Du, and Y. Jia, "Interval bipartite consensus of networked agents associated with signed digraphs," *IEEE Trans. Autom. Control*, vol. 61, no. 12, pp. 3755–3770, Dec. 2016.

[24] Y. Xu, R. Lu, H. Peng, K. Xie, and A. Xue, "Asynchronous dissipative state estimation for stochastic complex networks with quantized jumping coupling and uncertain measurements," *IEEE Trans. Neural Netw. Learn. Syst.*, vol. 28, no. 2, pp. 268–277, Feb. 2017.

[25] X. Song, J. Man, S. Song, and C. K. Ahn, "Gain-scheduled finite-time synchronization for reaction-diffusion memristive neural networks subject to inconsistent Markov chains," *IEEE Trans. Neural Netw. Learn. Syst.*, early access, Jul. 31, 2020, doi: 10.1109/TNNLS.2020.3009081.

[26] L. Zou, Z. Wang, H. Gao, and X. Liu, "State estimation for discrete-time dynamical networks with time-varying delays and stochastic disturbances under the round-robin protocol," *IEEE Trans. Neural Netw. Learn. Syst.*, vol. 28, no. 5, pp. 1139–1151, May 2017.

[27] L. Zhu, J. Qiu, and H. R. Karimi, "Region stabilization of switched neural networks with multiple modes and multiple equilibria: A pole assignment method," *IEEE Trans. Neural Netw. Learn. Syst.*, vol. 31, no. 9, pp. 3280–3293, Sep. 2020.

[28] X. Yang, Z. Feng, J. Feng, and J. Cao, "Synchronization of discrete-time neural networks with delays and Markov jump topologies based on tracker information," *Neural Netw.*, vol. 85, pp. 157–164, Jan. 2017.

[29] B. Liu and T. Chen, "Consensus in networks of multiagents with cooperation and competition via stochastically switching topologies," *IEEE Trans. Neural Netw.*, vol. 19, no. 11, pp. 1967–1973, Nov. 2008.

[30] X. Ge and Q.-L. Han, "Consensus of multiagent systems subject to partially accessible and overlapping Markovian network topologies," *IEEE Trans. Cybern.*, vol. 47, no. 8, pp. 1807–1819, Aug. 2017.

[31] Z. Meng, G. Shi, K. H. Johansson, M. Cao, and Y. Hong, "Behaviors of networks with antagonistic interactions and switching topologies," *Automatica*, vol. 73, pp. 110–116, Nov. 2016.

[32] S. Zhai and Q. Li, "Pinning bipartite synchronization for coupled nonlinear systems with antagonistic interactions and switching topologies," *Syst. Control Lett.*, vol. 94, pp. 127–132, Aug. 2016.

[33] L. Zhang, T. Yang, P. Shi, and Y. Zhu, *Analysis and Design of Markov Jump Systems with Complex Transition Probabilities*. Cham, Switzerland: Springer, 2016.

[34] J. Wang, J. Xia, H. Shen, M. Xing, and J. H. Park, "H_∞ synchronization for fuzzy Markov jump chaotic systems with piecewise-constant transition probabilities subject to PDT switching rule," *IEEE Trans. Fuzzy Syst.*, early access, Jul. 29, 2020, doi: 10.1109/TFUZZ.2020.3012761.

[35] H. Shen, F. Li, S. Xu, and V. Sreeram, "Slow state variables feedback stabilization for semi-Markov jump systems with singular perturbations," *IEEE Trans. Autom. Control*, vol. 63, no. 8, pp. 2709–2714, Aug. 2018.

[36] J. P. Hespanha, "Uniform stability of switched linear systems: Extensions of LaSalle's invariance principle," *IEEE Trans. Autom. Control*, vol. 49, no. 4, pp. 470–482, Apr. 2004.

[37] P. Tabuada, "Event-triggered real-time scheduling of stabilizing control tasks," *IEEE Trans. Autom. Control*, vol. 52, no. 9, pp. 1680–1685, Sep. 2007.

[38] D. Ye, M.-M. Chen, and H.-J. Yang, "Distributed adaptive event-triggered fault-tolerant consensus of multiagent systems with general linear dynamics," *IEEE Trans. Cybern.*, vol. 49, no. 3, pp. 757–767, Mar. 2019.

[39] T.-Y. Zhang and D. Ye, "Distributed secure control against denial-of-service attacks in cyber-physical systems based on K-connected communication topology," *IEEE Trans. Cybern.*, vol. 50, no. 7, pp. 3094–3103, Jul. 2020.

[40] W. He, T. Luo, Y. Tang, W. Du, Y.-C. Tian, and F. Qian, "Secure communication based on quantized synchronization of chaotic neural networks under an event-triggered strategy," *IEEE Trans. Neural Netw. Learn. Syst.*, vol. 31, no. 9, pp. 3334–3345, Sep. 2020.

[41] X. Li, Z. Sun, Y. Tang, and H. Karimi, "Adaptive event-triggered consensus of multi-agent systems on directed graphs," *IEEE Trans. Autom. Control*, vol. 66, no. 4, pp. 1670–1685, Apr. 2021.

[42] A. Girard, "Dynamic triggering mechanisms for event-triggered control," *IEEE Trans. Autom. Control*, vol. 60, no. 7, pp. 1992–1997, Jul. 2015.

[43] W. Hu, C. Yang, T. Huang, and W. Gui, "A distributed dynamic event-triggered control approach to consensus of linear multiagent systems with directed networks," *IEEE Trans. Cybern.*, vol. 50, no. 2, pp. 869–874, Feb. 2020.

[44] Q. Li, B. Shen, Z. Wang, and W. Sheng, "Recursive distributed filtering over sensor networks on Gilbert–Elliott channels: A dynamic event-triggered approach," *Automatica*, vol. 113, Mar. 2020, Art. no. 108681.

[45] Q. Li, B. Shen, Z. Wang, T. Huang, and J. Luo, "Synchronization control for a class of discrete time-delay complex dynamical networks: A dynamic event-triggered approach," *IEEE Trans. Cybern.*, vol. 49, no. 5, pp. 1979–1986, May 2019.

[46] F. Harary, "On the notion of balance of a signed graph," *Michigan Math. J.*, vol. 2, no. 2, pp. 143–146, 1953.

[47] Z. Wang, Y. Wang, and Y. Liu, "Global synchronization for discrete-time stochastic complex networks with randomly occurred nonlinearities and mixed time delays," *IEEE Trans. Neural Netw.*, vol. 21, no. 1, pp. 11–25, Jan. 2010.

[48] D. Meng, Z. Meng, and Y. Hong, "Uniform convergence for signed networks under directed switching topologies," *Automatica*, vol. 90, pp. 8–15, Apr. 2018.

[49] X. Liu, J. Cao, and C. Xie, "Finite-time and fixed-time bipartite consensus of multi-agent systems under a unified discontinuous control protocol," *J. Franklin Inst.*, vol. 356, no. 2, pp. 734–751, Jan. 2019.

[50] Y. Liu, Z. Wang, and X. Liu, "Global exponential stability of generalized recurrent neural networks with discrete and distributed delays," *Neural Netw.*, vol. 19, no. 5, pp. 667–675, Jun. 2006.

Jing Wang received the Ph.D. degree in power system and automation from Hohai University, Nanjing, China, in 2019.

She is currently an Associate Professor with the Anhui University of Technology, Ma'anshan, China. Her current research interests include Markov jump nonlinear systems, singularly perturbed systems, power systems, and nonlinear control.

Mengping Xing received the M.S. degree in electrical engineering from the Anhui University of Technology, Ma'anshan, China, in 2020. She is currently pursuing the Ph.D. degree with the School of Cyber Science and Engineering, Southeast University, Nanjing, China.

Her current research interests include persistent dwell-time switched systems, singularly perturbed systems, and robust control and filtering.

Jinde Cao (Fellow, IEEE) received the B.S. degree from Anhui Normal University, Wuhu, China, in 1986, the M.S. degree from Yunnan University, Kunming, China, in 1989, and the Ph.D. degree from Sichuan University, Chengdu, China, in 1998, all in mathematics and applied mathematics.

He is currently an Endowed Chair Professor, the Dean of the School of Mathematics, and the Director of the Research Center for Complex Systems and Network Sciences, Southeast University, Nanjing, China.

Prof. Cao is also a member of the Academy of Europe and the European Academy of Sciences and Arts, a fellow of the Pakistan Academy of Sciences, and an Academician of the International Academy for Systems and Cybernetic Sciences (IASCYS). He was a recipient of the Obada Prize, the National Innovation Award of China, and the Highly Cited Researcher Award in Engineering, Computer Science, and Mathematics by Thomson Reuters/Clarivate Analytics.

Ju H. Park (Senior Member, IEEE) received the Ph.D. degree in electronics and electrical engineering from the Pohang University of Science and Technology (POSTECH), Pohang, Republic of Korea, in 1997.

From May 1997 to February 2000, he was a Research Associate with the Engineering Research Center–Automation Research Center, POSTECH. He joined Yeungnam University, Gyeongsan, Republic of Korea, in March 2000, where he is currently the Chuma Chair Professor. He is a coauthor of the monographs *Recent Advances in Control and Filtering of Dynamic Systems with Constrained Signals* (New York, NY, USA: Springer-Nature, 2018) and *Dynamic Systems With Time Delays: Stability and Control (New York: Springer-Nature, 2019)* and an Editor of an edited volume *Recent Advances in Control Problems of Dynamical Systems and Networks* (New York: Springer-Nature, 2020). His research interests include robust control and filtering, neural/complex networks, fuzzy systems, multiagent systems, and chaotic systems. He has published a number of articles in these areas.

Prof. Park is also a fellow of the Korean Academy of Science and Technology (KAST). Since 2015, he has been a recipient of the Highly Cited Researchers Award by Clarivate Analytics (formerly, Thomson Reuters) and listed in three fields, Engineering, Computer Sciences, and Mathematics, in 2019 and 2020. He also serves as an Editor of the *International Journal of Control, Automation and Systems*. He is also a Subject Editor/Advisory Editor/Associate Editor/Editorial Board Member of several international journals, including *IET Control Theory & Applications, Applied Mathematics and Computation, Journal of The Franklin Institute, Nonlinear Dynamics, Engineering Reports*, *Cogent Engineering*, the IEEE TRANSACTIONS ON FUZZY SYSTEMS, the IEEE TRANSACTIONS ON NEURAL NETWORKS AND LEARNING SYSTEMS, and the IEEE TRANSACTIONS ON CYBERNETICS.

Hao Shen (Member, IEEE) received the Ph.D. degree in control theory and control engineering from the Nanjing University of Science and Technology, Nanjing, China, in 2011.

From 2013 to 2014, he was a Post-Doctoral Fellow with the Department of Electrical Engineering, Yeungnam University, Gyeongsan, Republic of Korea. Since 2011, he has been with the Anhui University of Technology, Ma'anshan, China, where he is currently a Professor. His current research interests include stochastic hybrid systems, complex networks, fuzzy systems and control, and nonlinear control.

Dr. Shen was a recipient of the Highly Cited Researcher Awards by Clarivate Analytics (formerly, Thomson Reuters) in 2019 and 2020. He has served on the technical program committee for several international conferences. He is also an Associate Editor/Guest Editor of several international journals, including *Journal of The Franklin Institute*, *Applied Mathematics and Computation*, *Neural Processing Letters*, and *Transactions of the Institute of Measurement and Control*.